Colloid and Polymer Science (2018) 296:1491–1499
https://doi.org/10.1007/s00396-018-4364-1

ORIGINAL CONTRIBUTION

Hydroxyapatite coated poly(lactic acid) microparticles with copper ion doping prepared via the Pickering emulsion route

Cho Yin Tham[1] · Wen Shyang Chow[1]

Received: 25 April 2018 / Revised: 5 June 2018 / Accepted: 25 June 2018 / Published online: 10 July 2018

Abstract

This work aimed to integrate the ionic substitution feature of hydroxyapatite nanoparticles (HAps) on poly(lactic acid) (PLA) surfaces. HAp-coated PLA microparticles were prepared through the Pickering emulsion route. HAps with adequate surface charge and aggregate size were prepared in a 0.1-M salt dispersion in order to induce oil-water interfacial adsorption of HAps in a Pickering emulsion. A batch sorption process was conducted to evaluate the potential of HAp-coated PLA microparticles to be loaded with copper ions. The concentration of Cu^{2+} in the supernatant phase was measured by atomic adsorption spectroscopy and their adsorption capacity was determined. The copper ion (Cu^{2+}) adsorption capacity of the microparticles increased with (a) the quantity of HAps adsorbed (consistently increased with HAp solid content) and (b) higher initial Cu^{2+} concentration of the doping medium. In conclusion, HAp-coated PLA microparticles with the ion doping feature were successfully prepared through the Pickering emulsion route.

Keywords Poly(lactic acid) · Hydroxyapatite · Microparticle · Emulsion

Introduction

In recent years, there has been increasing attention toward research on the incorporation of metallic ions in biomaterials as potential therapeutic agents. Among the metallic ions, copper (II) ion (Cu^{2+}) has demonstrated a beneficial effect in bone regenerative implant applications when incorporated within hydroxyapatite and other calcium phosphates. For antibacterial purposes, Cu^{2+}-doped hydroxyapatite exhibited a strong antimicrobial effect against *Escherichia coli* [1, 2]. In bone regeneration, it has been reported that the presence of Cu^{2+} effectively enhanced the activity and proliferation of osteoblastic cells [3, 4]. The presence of Cu^{2+} also enhanced the angiogenesis of a scaffold, a process of blood vessel formation which is of great importance in the healing of large bone defects [5]. Moreover, the solubility of hydroxyapatite showed improvement after the incorporation of 35% atomic content of Cu^{2+} [6].

PLA microparticles and nanoparticles are in high demand in biomedical applications, as they are capable of functioning as drugs depots and cell delivery systems with their advantage of injectable size [7]. Hydroxyapatite nanoparticles (HAps) have constantly been demonstrated to be an elegant inorganic-organic pair with PLA in biomaterials [8, 9]. Compositing HAps in a PLA polymeric matrix is the common approach to achieve synergistic improvement of mechanical properties, bioactivity, and lowering inflammatory response when alkaline HAps neutralize the acid degradation products of PLA [10–12]. However, the ion substitution feature of HAps becomes non-functional when HAps are dispersed and embedded within polymer matrices. It is well known that the calcium ions in the hydroxyapatite chemical structure ($Ca_5(OH)(PO_4)_3$) are readily active to be replaced by other cations through the synthesis route [13], bulk absorption [5], and surface ion-exchange mechanisms [6]. The surface ion-exchange mechanism facilitates the post-doping on HAps with other metallic ions that could greatly expand the versatility in the design of biomaterials. It will be more valuable to coat a layer of HAps on PLA surfaces rather than solely mixing both materials into a monolithic composite.

A particle-stabilized emulsion, also known as a Pickering emulsion, is used to describe an immiscible liquid-liquid mixture system stabilized by colloidal particles [14]. Colloidal

✉ Wen Shyang Chow
shyang@usm.my

[1] School of Materials and Mineral Resources Engineering, Engineering Campus, Universiti Sains Malaysia, Nibong Tebal, 14300 Penang, Malaysia

particles adsorbed on emulsion droplet interfaces tend to reduce the interfacial energy and provide kinetic stability to the emulsion system [15–17]. The applications of Pickering emulsions have broadened in the biomedical field due to the marked advantage in surfactant-free preparation processes [18]. Substitution of surfactants with colloidal particles as emulsion stabilizers can potentially eliminate the toxicology issues provoked by residual surfactant. Furthermore, the assembly of colloidal particles on the outer layer enables us to give an additional functionality to the coated material.

In this study, it is intended to apply a Pickering emulsion to prepare HAp-coated PLA microparticles. Herein, the colloidal dispersion of HAps is present as a continuous phase in the emulsion system. The dispersion behavior of HAps would greatly affect the formation of a stable Pickering emulsion and further their attachment to microparticle surfaces. Our recent report [19] demonstrated the importance of HAp surface charges in controlling the HAp attachment to particle surfaces and consequently affecting the morphologies of PLA particles. In this report, the effects of salt concentration and HAp solid content in a Pickering emulsion on PLA microparticle formation were investigated. A comprehensive view is provided on the application of the Pickering emulsion in microparticle fabrication processes through micrographic images and particle size analysis. Further, the potential of doping the HAp-coated PLA surfaces with copper ions (Cu^{2+}) was demonstrated.

Materials and methods

Materials

Hydroxyapatite nanoparticles (HAps) were purchased from Sigma-Aldrich (chemical structure of $Ca_5(OH)(PO_4)_3$, particle size < 200 nm, and specific surface area > 20.2 m^2/g from Brunauer-Emmer-Teller (BET) analysis, and 38.9% Ca^{2+} measured from complexometric titration). Poly(lactic acid) (PLA) was supplied from NaturalWork®, grade 3150D (0.2% D-lactide content and molecular weight M_w of 93,500 g/mol, specific gravity 1.25 g/cm^3). Potassium nitrate (KNO_3) and dichloromethane (DCM) were purchased from Merck Millipore. Copper (II) nitrate ($Cu(NO_3)_2$) from Sigma-Aldrich was used as the source of copper ions (Cu^{2+}). All aqueous solutions were prepared with deionized water produced by an Elga® Purelab® Flex 3 water purification system.

Preparation of HAp-coated PLA microparticles

HAp-coated PLA microparticles were prepared by a Pickering emulsion and solvent removal method. The oil-in-water emulsion was obtained by dispersing a dichloromethane solution with 5 wt% PLA in HAp dispersions with concentrations varied from 0.001 to 0.1 wt%. Prior to emulsification, HAps were dispersed in water by means of probe sonication (QSonica Q700) at an amplitude of 70% for 60 s in an ice bath). The ionic strength of the HAp dispersion was adjusted by dissolving the KNO_3 salt in a concentration range from 0.01 to 1.0 M. It is known that KNO_3 is a type of electrolyte which can be used to control the ionic strength level of an aqueous dispersion. The surface charge density, double-layer repulsion, and the aggregation behavior of HAp could be controlled by adjusting the ionic strength in aqueous dispersion using KNO_3. The volume ratio of the oil:water phase of the emulsion was set at 1:7, in which the dispersed phase attributed to 25 ml and the continuous phase attributed to 175 ml in a total of 200 ml. Emulsification was conducted by a mechanical overhead stirrer (Heidolph RZR 2041) at a speed of 1300 rpm for 5 min. Subsequently, the emulsion was continuously stirred for 12 h at a speed of 70 rpm to allow solvent removal and precipitation of solid microparticles. Microparticles were collected by filtration and washed with deionized water followed by drying with silica gel.

Characterizations

The surface potential (measured as the zeta potential) and hydrodynamic size of the HAp dispersion were characterized by a Nano ZetaSizer ZS (Malvern Instrumental Ltd.). HAp dispersions were prepared at a dilute concentration of 0.001 wt% solid content to avoid multiple-scattering effects. The HAps were dispersed by probe sonication (70% amplitude, 60 s) prior to testing at 25 °C. A polarized optical microscope (Meiji Techno MT8000 series) was used to observe HAp dispersions with varied particle concentrations (0.005–0.1 wt%).

Once the emulsification step was complete, the emulsion droplets were observed by an optical microscope, and the average diameter was estimated by counting 500 droplets. The size of PLA microparticles was characterized by a MasterSizer 3000 (Malvern Instrumental Ltd.), and the average particle size was taken as the Sauter mean diameter. The structural morphology of PLA microparticles was observed using field emission scanning electron microscopy (Carl Zeiss FE-SEM, Supra 55-VP, operating at 3 kV). Prior the FESEM, PLA microparticles were sputtered with a gold conductive layer (Bio-Rad Laboratories, Polaron Division, at 0.1 mbar and 5 mA for 600 s). For PLA particles with sizes > 1 mm, the morphology was observed by a stereo zoom optical microscope (Kunoh-Robo).

Fourier transform infrared (FTIR Model PE 4000 series, PerkinElmer Cetus Instrument) spectroscopy was used to analyze the chemical structure of HAp-coated PLA microparticles. Microparticles were dried in an oven at 45 °C for 24 h prior to analysis. During analysis, microparticles were

dispersed in potassium bromide and compressed into a thin film. The spectral resolution was set at 4 cm^{-1}, and the scanning range was set from 400 to 4000 cm^{-1}.

The amount of HAps coated onto the microparticles was quantitatively determined by thermogravimetric analysis (TGA; PerkinElmer Pyris 6, nitrogen atmosphere 20 mL/min). The sample was heated from 30 to 500 °C at a heating rate of 10 °C/min. The amount of adsorbed HAp (mg/g) was estimated from Eq. (1), where M_i is the initial mass of HAp-coated PLA microparticles and M_r is the residual mass remaining after the complete decomposition of the PLA component.

$$\text{Amount of adsorbed HAps} = M_r/M_i \quad (1)$$

A batch sorption process was conducted to serve as the preliminary study in determining the potential of HAp-coated PLA microparticles to be loaded with metallic ions. Copper ion (Cu^{2+}) served as the adsorbate. A stock Cu^{2+} solution with a concentration of 1000 ppm was prepared and further diluted to initial concentrations of 10 and 50 ppm for the sorption test. A sample of 100 ± 5 mg was immersed in 20 mL of Cu^{2+} solution and continuously shaken at 350 rpm for 48 h in an incubator (Heidolph Unimax 1010) at 37 °C until equilibrium adsorption was reached. Microparticles were separated from the Cu^{2+} solution by glass wool filtration. Further, the concentration of Cu^{2+} in the supernatant phase was measured by atomic adsorption spectroscopy (PerkinElmer AA800, the flame of air-acetylene gases, Cu^{2+} atomic adsorption at $\lambda = 324.8$ nm). All samples were measured in triplicate. The amount of the Cu^{2+} ion adsorbed on the PLA microparticles was determined according to Eq. (2):

$$\text{Adsorption Capacity}, q_m = [(C_o - C)V]/m \quad (2)$$

where q_m (mg/g) is the maximum amount of Cu^{2+} adsorption per unit mass of microparticles in equilibrium. The C_o is the initial concentrations of the Cu^{2+} ions in the initial solution and C is the concentration of Cu^{2+} ions in the aqueous phase after the sorption process, V (mL) is the volume of the Cu^{2+} solution, and m (g) is the amount of HAp-coated PLA microparticles.

Results and discussion

HAp dispersion:salt concentration and HAp solid content

Figure 1 shows the zeta potential, mean particle size, and the particle size distribution of HAp dispersions with varied salt concentration. In the absence of salt, pristine HAps had the highest zeta potential magnitude of − 32.7 mV and a minimum mean particle size of 196.4 nm. The SEM micrograph illustrated that the pristine HAps are in the state of primary aggregation. The results showed that the magnitude of zeta potential decreased from − 21.3 to − 0.05 mV as the salt concentration increased. Meanwhile, the mean particle size of HAps increased from 366.2 to 1287 nm. From the particle size distribution curves, it is observed that the single peak curve of pristine HAps has split into a bimodal curve after the addition of salt. These bimodal curves consisted of the two major peaks, wherein the first peak was located at the lower particle size range of < 100 nm and second peak shifted to a larger particle size range when the salt concentration increased. At 0.1 M, the particle size distribution curve of HAps contained a shoulder on the left side of the curve instead of a distinct bimodal curve shape compared to 0.01 and 1.0 M salt concentrations. These results might suggest that the amount of salt in HAps dispersion affecting the electrostatic repulsive suppression between particles and particle aggregates differently, which further leads to different aggregation behaviors and hence the particle size distribution of

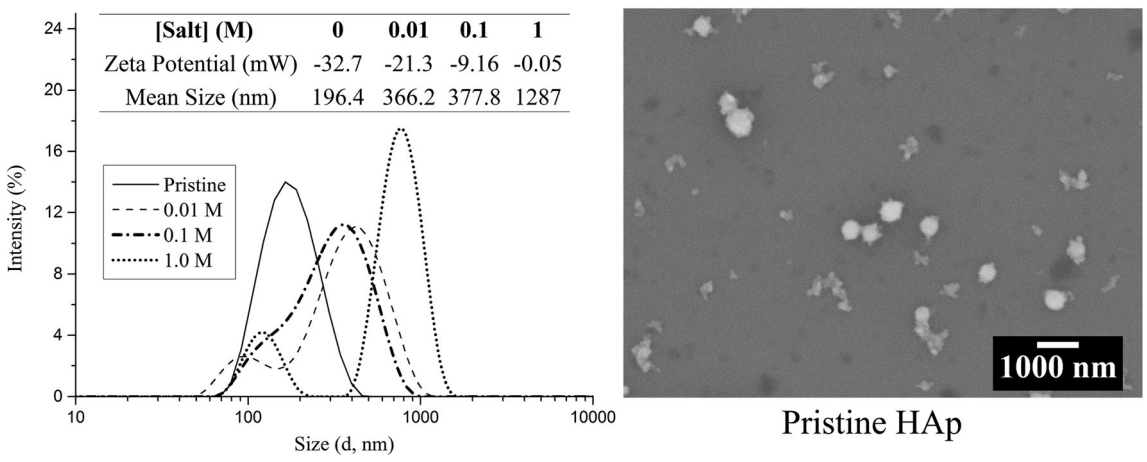

Fig. 1 Effect of salt concentration on the 0.001 wt% HAp dispersion

HAps. As the salt concentration increases, the negative surface potential of the HAp might be suppressed by the Debye screening effect that reduces the thickness of the electrical double layer. The suppression of the double layer reduces the repulsive forces between particles, further induces the flocculation of particles and lead to the increases of HAp size. Typically, HAps had negatively charged surfaces due to the formation of surface complexes through the hydrolysis mechanism. To function as a particle stabilizer in the emulsion, HAps are not favored to adsorb firmly on the oil-water interface. Their surface hydrophilicity (attributed to surface charges) and nanosize would give rise to low attachment energy comparable with thermal energy, and this could lead to reversible adsorption-desorption of the particle at the interface. Furthermore, their negatively charged surface can cause them to be repelled from the negatively charged oil-water interface [20, 21]. According to Marinova et al. [20], the bare oil-water interface is negatively charged by the adsorption of hydroxyl (OH^-) ions. The hydroxyl ion is released through the dissociation-association equilibrium of the water molecules. The reduction of zeta potential demonstrated that the HAp surface charge magnitude and particle size could be adjusted by varying the salt concentration in the dispersing medium. In the following studies, the salt concentration of 0.1 M was selected due to the adequate surface charge magnitude and mean particle size of HAp.

Figure 2 shows the aggregation behavior of HAps with the increased HAp solid content at 0.1 M salt. From the observation, the HAps were evenly distributed throughout the dispersion at the low solid content. As the HAp solid content increased, particles showed a higher tendency to aggregate and form network structures. Generally, at a fixed salt concentration, the energy barrier between particles is fixed. The number of particles with sufficient energy to overcome the energy barrier increases with HAp solid content, further inducing particle aggregation. This phenomenon is known as diffusion-limited colloid aggregation. This phenomenon occurs when there is a negligible repulsive force between the colloid particles in the presence of salt, and the aggregation rate is limited solely by the time taken for particle clusters to encounter each other by diffusion. Moreover, with the increases of particle concentration, the collision frequency between particles increases, consequently enhancing the particle aggregation in the dispersion [22, 23].

Preparation of HAp-coated PLA microparticles

The effects of HAp solid content on droplets and microparticle preparation were investigated. Figure 3 illustrates the emulsion droplets stabilized by HAp at varied solid content levels. The average diameter of an emulsion droplet and the Sauter Mean diameter of the PLA microparticles are shown in Fig. 4. The disparity between the droplet and microparticle size was observed at HAp solid contents < 0.05 wt%. From Fig. 4, the morphology transformation of PLA microparticles from beads to spheres and to deflated spheres was observed with the increased HAp solid content. In addition to that, the surface morphology of deflated spheres and spherical microparticles was demonstrated.

Droplet formation and particle stabilization of the Pickering emulsion typically follow the sequences of (1) oil phase fragmentation, (2) particle stabilizer and droplet collision, and (3) effective particle interfacial adsorption. The efficiency of oil phase fragmentation determines the amount of the oil-water interface generated in the emulsion system. The results in Fig. 4 show that the average droplet size was relatively consistent throughout the HAp solid contents in the dispersion. This suggests that the emulsification efficiency of the fabrication process is independent of the HAp solid content in the emulsion.

In the emulsification process, the adsorption of HAps on droplet interfaces is dependent on the collision event between HAps and PLA droplets. The collision mechanism is typically driven by the fluctuating turbulence of the aqueous phase. Effective collision leads to the effective interfacial adsorption and thus droplet stabilization. In general, the increases of particle solid content would increase the particle-droplet collision frequency and thus enhance the effectiveness of particle interfacial adsorption [24]. The adsorption of HAps on the droplet surface can be clearly viewed in Fig. 3, wherein the droplet

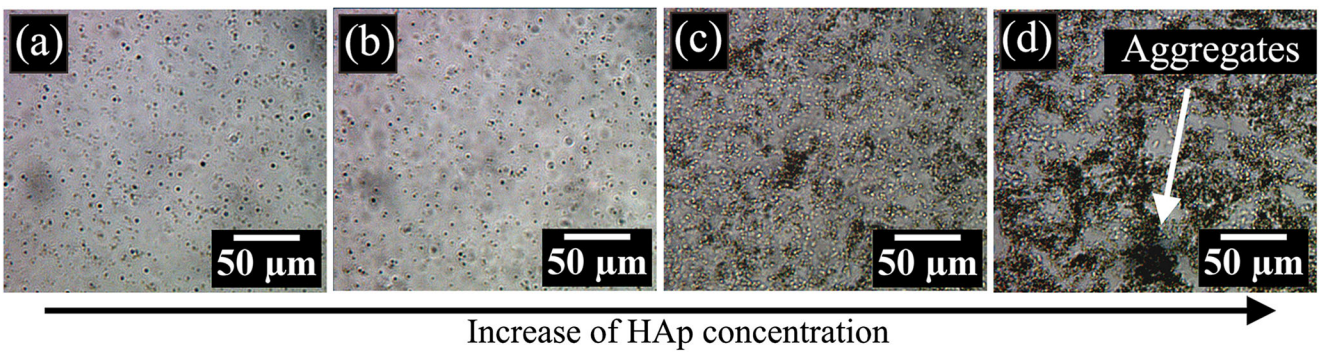

Fig. 2 HAp dispersions with solid contents of **a** 0.005, **b** 0.01, **c** 0.05, and **d** 0.1 wt% at 0.1 M salt

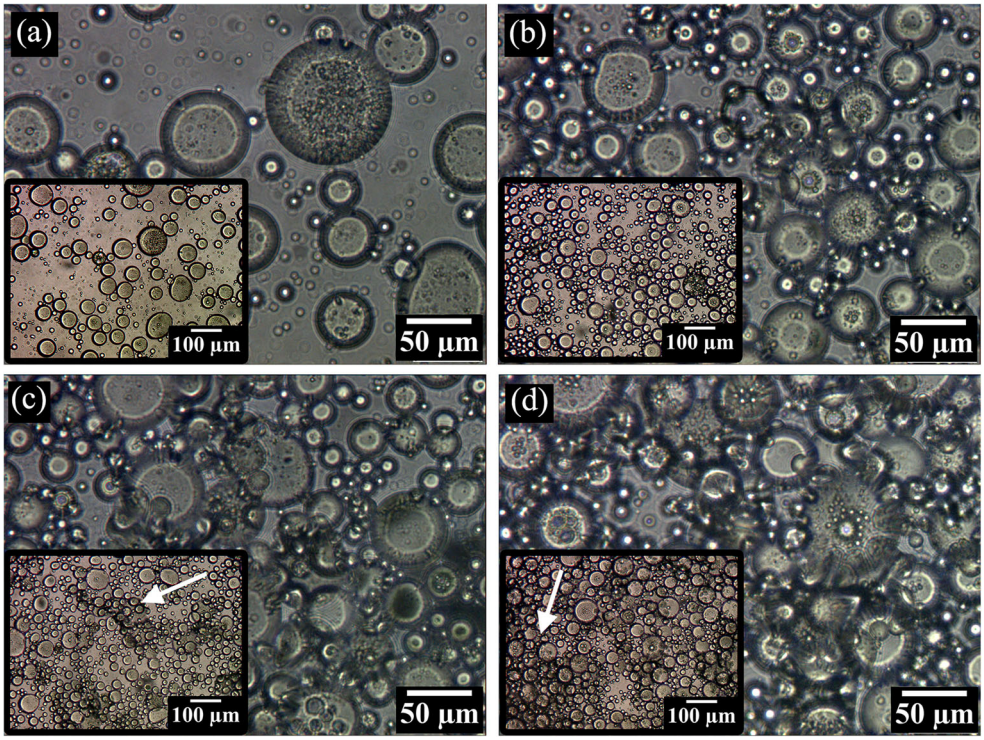

Fig. 3 Emulsion droplets prepared from different HAp solid contents at **a** 0.005, **b** 0.01, **c** 0.05, and **d** 0.1 wt% with 0.1 M salt. The presence of HAp aggregates are indicated by the white arrow in **c**, **d**

appeared spherical and fairly polydisperse. At the lowest HAp solid content, 0.005 wt% (Fig. 3a), the droplets were discretely dispersed in the medium. However, it is noted that the small oil droplets were absent when compared to Fig. 3b–d. These results suggest the occurrence of ripening destabilization when droplets were stabilized at 0.005 wt% HAp. According to Juárez and Whitby [22], when the emulsion is stabilized under a low particle solid content, the droplet with low particle surface coverage potentially undergoes Ostwald ripening destabilization during the early stage of emulsion destabilization. Ostwald ripening destabilization is controlled by the molecular solubility of the oil in the aqueous phase. The oil molecules transfer from small to large drops due to their different Laplace pressures. As the HAp solid content increases in the emulsion system, the tendency of limited-diffusion colloid aggregation of HAp enhances (cf. Fig. 2). The presence of HAp aggregates in the emulsion system potentially densifies the amount of HAp adsorbed on droplet interfaces. In turn, the ripening destabilization might be diminished when sufficient particles adsorb on the interfaces, subsequently impeding the coalescing of droplets even in close contact with each other.

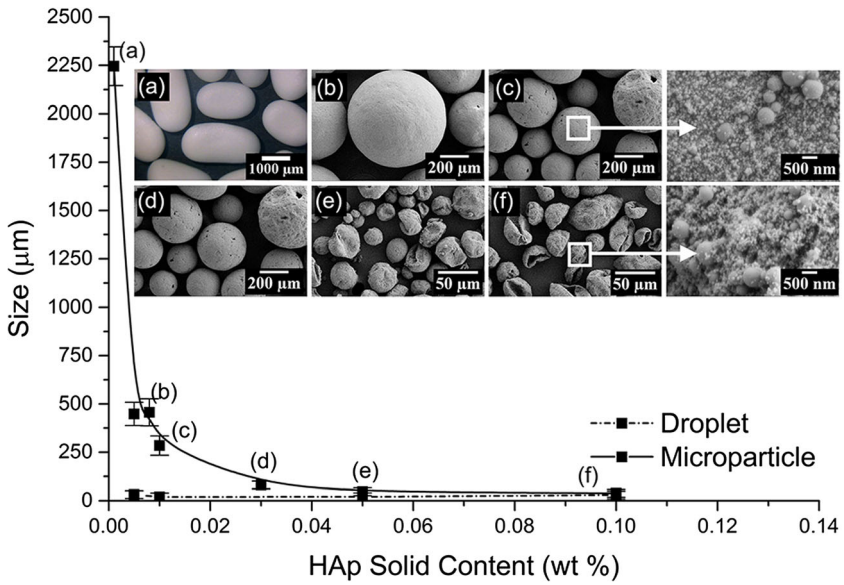

Fig. 4 The line graph showed the size of the PLA droplet and microparticle prepared from different HAp solid contents; the SEM micrographs revealed the structural and surface morphology of PLA microparticles from corresponding HAp solid contents

After emulsification is complete, the solvent removal process is expected to follow an ideal mechanism: (1) the solvent exiting isotopically from polymer droplets through diffusion, (2) isotropic shrinkage of droplets, and (3) formation of the spherical microparticle. From the structural morphology of microparticles revealed in Fig. 4, these results suggest that the solvent removal of droplets did not follow the common ideal mechanism. PLA beads were formed at 0.001 wt% HAp, whereas PLA microparticles with spherical morphology were obtained at 0.008 and 0.01 wt% HAp. As the HAp solid content further increased beyond 0.03 wt%, the deflated-sphere microparticles were obtained. Parallel with the transformation of structural morphologies, the microparticle size of PLA decreased exponentially with the increased HAp solid content. The variation in microparticle morphology and size suggests that the stability of droplets varied with HAp solid content in the emulsion, where the stability might depend on the coverage of HAps on the droplet interface. During solvent removal, the droplet will become more viscous and tacky. If the particle coverage on droplets is insufficient, droplets tend to coalescence upon collision, consequently affecting the size and morphology of the microparticle [25]. Arditty et al. [15] described the destabilization of droplets under insufficient surface coverage as a limited-coalescence phenomenon. When the interface produced by emulsification fragmentation is larger than the coverage capacity of the particles, the partially covered droplets will continuously coalescence and merge to minimize the interface area. Finally, the process will halt when the interface is covered by a monolayer of particles.

The concept of the limited-coalescence phenomenon is supported by the observation of the surface morphology of the PLA microparticles. The surfaces of spherical microparticles revealed in Fig. 4c were covered with a layer of HAps with homogenous thickness. Furthermore, the spherical microparticles were larger compared to the droplets due to the merging upon coalescence. In contrast, the surfaces of the deflated-sphere microparticles (Fig. 4f) were covered with a relatively thick and aggregated layer of HAps. Their small particle size suggests that the HAp-coated interfaces prevent the coalescence and merging of droplets. Furthermore, the heavily coated interfaces might offer substantial rigidity to droplet surfaces, consequently increasing the resistivity of isotropic shrinkage on droplets during solvent removal. The interfacial tension on the droplet surfaces during shrinkage collapses the spherical structure of the droplet and forms deflated-sphere microparticles [16].

Figure 3c, d reveals the presence of HAp aggregates (see the white arrow) in the emulsion. The presence of HAp aggregates suggests that the emulsion system might contain excess HAps that have not been consumed in the interfacial adsorption. Since the emulsification efficiency is constant, the amount of HAps incorporated into the emulsion system might be beyond the quantity demanded to stabilize the oil-water interfaces. Meanwhile, the results in Figure 4 show that there was a large size disparity between droplet and microparticle until the HAp solid content increased beyond 0.05 wt%, where the plateau zone was reached and the microparticle and the droplet were of comparable sizes. Reaching the plateau zone for HAp content beyond 0.05 wt% suggests that excess HAps might have improved the droplet stability against coalescence. Hence, the highest stability of the Pickering emulsion is achieved at 0.1 wt% HAp solid content.

Characteristics of HAp-coated PLA microparticles

Figure 5 shows the FTIR absorption spectrum of pristine HAp, pristine PLA, and microparticles, respectively. In the pristine HAp spectrum, there are three distinct bands originating from the stretching vibrations of PO_4 groups at 1047, 601, and 570 cm^{-1}. The sharp bands at 3570 and 632 cm^{-1} correspond to the OH stretching and bending modes of the HAps, respectively. In contrast, the broad absorption band centered at 3435 cm^{-1} and the band located at 1630 cm^{-1} were attributed to the O–H stretching vibration of adsorbed water. For pristine PLA, the absorption band of the carbonyl group (C=O) is located to 1750 cm^{-1}, and the C–H bonds of the methyl group of PLA are located at 2993 and 2945 cm^{-1}. The characteristic peaks of the microparticle spectrum revealed a combination of both pristine HAps and PLA.

On the other hand, the amount of HAps adsorbed on the PLA microparticle was determined by means of TGA, as shown in Fig. 6. From the results, pristine PLA showed complete disintegration at temperatures > 400 °C. The onset of microparticle decomposition was consistent with pristine PLA at 321.2 °C, and the remaining weight of 12.29% at 500 °C. The residual weight was attributed to

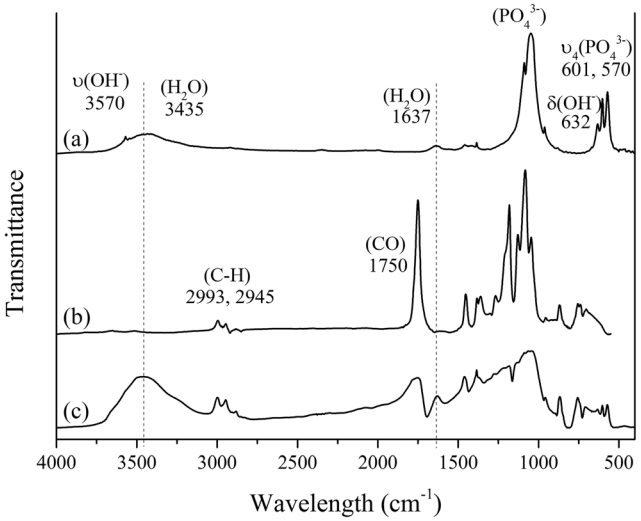

Fig. 5 FTIR spectrum of **a** pristine HAps, **b** pristine PLA, and **c** HAp-coated PLA microparticles

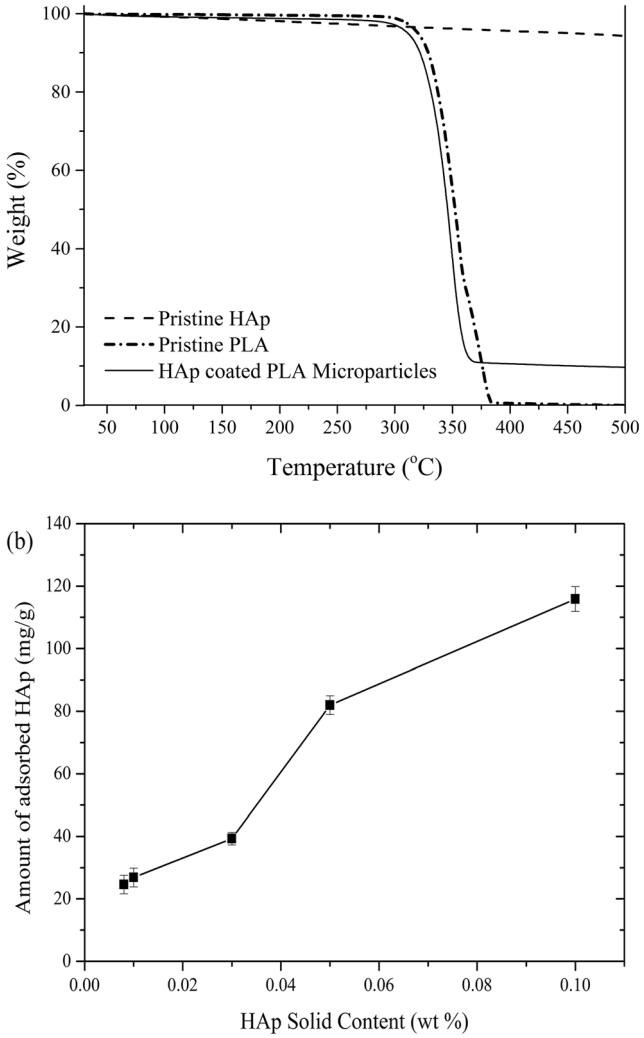

Fig. 6 **a** Thermogravimetric analysis of HAp-coated PLA microparticles and **b** the amount of adsorbed HAps (mg/g) prepared from varied HAp solid contents in the Pickering emulsion

the presence of HAps. In pristine HAps, there was a continuous weight loss up to 5.88% when the temperature increased to 500 °C. This result was consistent with the studies reported by Holmes and Beebe [26], which indicated that the weight loss of hydroxyapatite of approximately 3 to 7% was attributed to the removal of moisture from the surface when heated to 500 °C. On the other hand, Fig. 6b shows the amount of adsorbed HAps (mg/g) prepared at varied HAp solid contents in the Pickering emulsion. The amount of adsorbed HAps increased from 24.6 to 115.8 mg/g, consistent with the increased HAp solid content in the emulsion. These results indicated that the amount of HAps adsorbed on PLA surfaces could be controlled by adjusting the HAp solid content in the Pickering emulsion, successively adjusting the metal ion adsorption capacity of PLA microparticles, as demonstrated in the following Cu^{2+} adsorption studies.

The general mechanisms of Cu^{2+} adsorption on HAps are known to be induced by a combination of ion exchange with Ca^{2+} of the HAp lattice and the formation of surface complexation with the P–OH groups of the HAp lattice [27]. Figure 7 shows the Cu^{2+} adsorption capacity of HAp-coated PLA microparticles. Overall, the adsorption capacity of PLA microparticles increased with (a) more adsorbed HAps on the surfaces (which increased consistently with the HAp solid content in the emulsion) and (b) a higher initial Cu^{2+} concentration of the immersed solution. Since the metallic ion binding site is present in the HAp chemical structure, it is thus reasonable that the adsorption capacity increased with HAps attached to PLA surfaces. In contrast, for the latter, the ratio of Cu^{2+} to the number of available adsorption sites of HAps is controlled by the initial Cu^{2+} concentration. When the Cu^{2+} concentration increased, a constant mass of the microparticle was exposed to a larger quantity of metal ions. Progressively, a higher number of metal ions were available to be taken up by the appropriate binding sites on the HAp, which thus increased the adsorption capacity of the microparticles. In addition, a higher Cu^{2+} concentration was able to increase the adsorption capacity due to a greater driving force induced by the concentration gradient [28]. These results further suggested the possibility to control the quantity of Cu^{2+} to be doped on the PLA microparticles by changing the initial concentration of Cu^{2+} in the immersion solution. Similarly, Vitale-Brovarone et al. [29] had reported the feasibility of modulating the amount of adsorbed metal ions onto the scaffold by tuning the parameters that control the ion-exchange process, e.g., metallic ion concentration, time, and temperature.

Table 1 summarizes the studies in the literature where the Cu^{2+} ions were incorporated into the hydroxyapatite- and calcium phosphate-based biomaterials. Since the effective

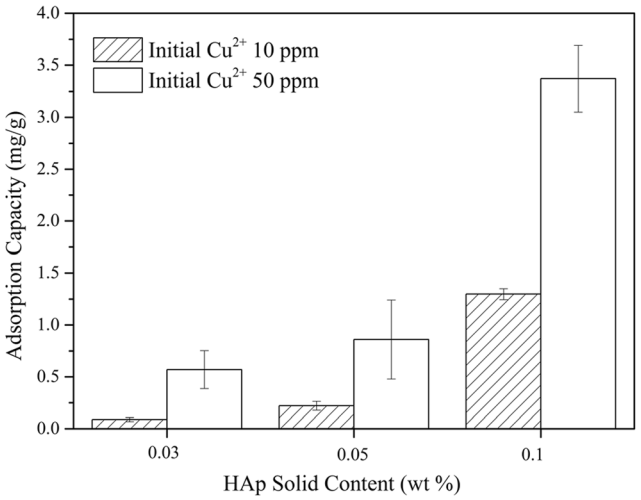

Fig. 7 Copper ion (Cu^{2+}) adsorption capacity of HAp-coated PLA microparticles prepared from varied HAp solid contents in the Pickering emulsion

Table 1 The quantity of copper ion (Cu^{2+}) incorporated in hydroxyapatite and calcium phosphate biomaterials

Material	Quantity of Cu^{2+}	Ref.
Hydroxyapatite coated biomaterial substrate		
Hydroxyapatite nanoparticle coated poly(lactic acid) microparticle	1.29 and 3.37 mg/g	Current studies
Hydroxyapatite coated on titanium alloy	0.8 wt% Cu^{2+},with the degree of Cu^{2+} substitution of Ca^{2+} with x = 0.025 for Cu-hydroxyapatite ($Ca_{10-x}Cu_x(PO_4)_6(OH)_2$)	[1]
Hydroxyapatite and others calcium phosphate		
Hydroxyapatite powder	0.66 and 3.3 wt% or 0.0105 and 33 mg/g	[2]
Calcium phosphate films	0.03 to 1.37 μg per sample or 3×10^{-5} to 1.37×10^{-3} mg per sample	[3]
Calcium phosphate cement, brushite ($CaHPO_4.2H_2O$)	0.056, 0.56, and 5.65 μg Cu^{2+}/cm^2	[4]
Dicalcium phosphate dehydrate	22 and 220 ng of Cu^{2+} per scaffold (with dimension 8 × 8 × 2 mm)	[5]
Hydroxyapatite granules	0.35% Cu^{2+} atomic content divalent Ca^{2+} substitution in hydroxyapatite	[6]

therapeutic or toxic concentrations of Cu^{2+} have yet to be determined, it is noticeable that the amount of Cu^{2+} being incorporated into the biomaterial was varied. Therefore, ASTM F1185–03 and ASTM F1088-04a have addressed this by specifying the limits of toxic and heavy metals in hydroxyapatite and resorbable calcium phosphate surgical implants, respectively [30, 31]. Accordingly, the maximum allowable limit of Cu^{2+} is 50 ppm. In this study, the amount of Cu^{2+} doped from 50 ppm Cu^{2+} solutions was 3.37 mg/g, which is below the allowable limit mentioned in ASTM.

From the summary in Table 1, it is noticeable that the works conducted on doping the Cu^{2+} on calcium phosphate-based materials were generally in the form of granules, powders, or scaffolds. These biomaterials are commonly prepared through granulation from bulk materials, precipitation from synthesis, and solvent-casting methods. The application of the Pickering emulsion in preparing particulates with an ion-doping capability has not yet been reported elsewhere. Furthermore, the application of the Pickering emulsion allows the coating of nanoparticles on microparticle surfaces consisting of materials of different types, such as, in this report, the pairing of calcium phosphate ceramic with a biodegradable polymer. As shown in Table 1, the HAp-coated PLA microparticle had the advantage of doping larger amounts of Cu^{2+} ions compared to others. This might result from the larger surface area of HAps attached to PLA microparticles and, in turn, more binding sites available for metallic ion doping.

Conclusions

HAp-coated PLA microparticles were prepared by a Pickering emulsion and solvent removal method. The HAp dispersion has replaced conventional surfactant and acted as a particle stabilizer in the emulsion. The salt concentration of the HAp dispersion was fixed at 0.1 M due to the adequate surface charges and aggregate size of the HAp for oil-water interfacial adsorption. As the HAp solid content increased in the emulsion, the microparticle size decreased exponentially and the structural morphology transformed from beads to spheres and to deflated spheres. A HAp 0.1 wt% solid content dispersion provided optimum stability to the Pickering emulsion against coalescence destabilization, supported by the results of microparticle size and consistent with emulsion droplet size. The amount of HAps attached to PLA microparticles surfaces increased with the HAp solid content in the Pickering emulsion and thus increased the Cu^{2+} adsorption capacity of the PLA microparticles. In summary, the intention to prepare HAp-coated PLA microparticles with the metallic ion substitution feature is achieved.

Acknowledgements We gratefully acknowledged the financial support provided by Research University grant (RUI, 1001/PBAHAN/814199) from Universiti Sains Malaysia.

Funding This study was funded by Universiti Sains Malaysia (grant number RUI, 1001/PBAHAN/814199).

Compliance with ethical standards

Conflict of interest The authors declare that they have no conflict of interest.

References

1. Huang Y, Zhang X, Zhao R, Mao H, Yan Y, Pang X (2015) Antibacterial efficacy, corrosion resistance, and cytotoxicity studies on copper-substituted carbonated hydroxyapatite coating on titanium substrate. J Mater Sci 50(4):1688–1700

2. Li Y, Ho J, Ooi CP (2010) Antibacterial efficacy and cytotoxicity studies of copper (II) and titanium (IV) substituted hydroxyapatite nanoparticles. Mater Sci Eng C 30(8):1137–1144
3. Yang L, Perez-Amodio S, FYFB-d G, Everts V, Blitterswijk CAC, Habibovic P (2010) The effects of inorganic additives to calcium phosphate on in vitro behavior of osteoblasts and osteoclasts. Biomaterials 31:2976–2989
4. Ewald A, Käppel C, Vorndran E, Moseke C, Gelinsky M, Gbureck U (2012) The effect of Cu(II)-loaded brushite scaffolds on growth and activity of osteoblastic cells. J Biomed Mater Res A 100(9): 2392–2400
5. Barralet J, Gbureck U, Habibovic P, Vorndran E, Gerard C, Doillon CJ (2009) Angiogenesis in calcium phosphate scaffolds by inorganic copper ion release. Tissue Eng A 15(7):1601–1609
6. Lima IRD, Alves GG, Soriano CA, Campaneli AP, Gasparoto TH, Junior ESR, Sean LÁD, Rossi AM, Granjeiro JM (2011) Understanding the impact of divalent cation substitution on hydroxyapatite: an in vitro multiparametric study on biocompatibility. J Biomed Mater Res A 98A:351–358
7. Ho ML, Fu YC, Wang GJ, Chen HT, Chang JK, Tsai TH, Wang CK (2008) Controlled release carrier of BSA made by W/O/W emulsion method containing PLGA and hydroxyapatite. J Control Release 128(2):142–148
8. Zhu Y, Wang Z, Zhou H, Li L, Zhu Q, Zhang P (2017) An injectable hydroxyaptite/poly(lactide-co-glycolide) composites reinforced by micro/nano-hybrid poly(glycolide). Mater Sci Eng C 80:326–334
9. Nagata F, Miyajima T, Kato K (2016) Preparation of phylloquinone-loaded poly(lactic acid)/hydroxyapatite core-shell particles and their drug release behavior. Adv Powder Technol 27(3):903–907
10. Wang X, Song G, Lou T (2010) Fabrication and characterization of nano composite scaffold of poly(L-lactic acid)/hydroxyapatite. J Mater Sci Mater Med 21(1):183–188
11. Danoux CB, Barbieri D, Yuan H, Bruijn JDD, Blitterswijk CAV, Habibovic P (2014) In vitro and in vivo bioactivity assessment of a polylactic acid/hydroxyapatite composite for bone regeneration. Biomatter 4(1):e27664
12. Rakmae S, Ruksakulpiwat Y, Sutapun W, Suppakarn N (2012) Effect of silane coupling agent treated bovine bone based carbonated hydroxyapatite on in vitro degradation behavior and bioactivity of PLA composites. Mater Sci Eng C 32(6):1428–1436
13. Trinkunaite-Felsen J, Prichodko A, Semasko M, Skaudzius R, Beganskiene A, Kareiva A (2015) Synthesis and characterization of iron-doped/substituted calcium hydroxyapatite from seashells *Macoma balthica* (L.). Adv Powder Technol 26(5):1287–1293
14. Chevalier Y, Bolzinger M-A (2013) Emulsions stabilzed with solid nanoparticles: Pickering emulsion. Colloids Surf A Physicochem Eng Asp 439:23–34
15. Arditty S, Whitby CP, Binks BP, Schmitt V, Leal-Calderon F (2003) Some general features of limited coalescence in solid-stabilized emulsions. Eur Phys J E Soft Matter 11(3):273–281
16. Okada M, Maeda H, Fujii S, Nakamura Y, Furuzono T (2012) Formation of Pickering emulsions stabilized via interaction between nanoparticles dispersed in aqueous phase and polymer end groups dissolved in oil phase. Langmuir 28(25):9405–9412
17. Zhang M, Wang A-j, J-m L, Song N, Song Y, He R (2017) Factors influencing the stability and type of hydroxyapatite stabilized Pickering emulsion. Mater Sci Eng C 70:396–404
18. Wei Z, Wang C, Liu H, Zou S, Tong Z (2012) Facile fabrication of biocompatible PLGA drug-carrying microspheres by Pickering emulsions. Colloids Surf, B Biointerfaces 91:97–105
19. Tham CY, Chow WS (2017) Poly(lactic acid) microparticles with controllable morphology by hydroxyapatite stabilized Pickering emulsions: effect of pH, salt and amphiphilic agents. Colloids Surf A Physicochem Eng Asp 533:275–285
20. Marinova KG, Alargova RG, Denkov ND, Velev OD, Petsev DN, Ivanov IB, Borwankar R (1996) Charging of oil-water interfaces due to spontaneous adsorption of hydroxyl ions. Langmuir 12(8): 2045–2051
21. Lin Y, Böker A, Skaff H, Cookson D, Dinsmore AD, Emrick T, Russell TP (2005) Nanoparticle assembly at fluid interfaces: structure and dynamics. Langmuir 21(1):191–194
22. Juárez JA, Whitby CP (2012) Oil-in-water Pickering emulsion destabilisation at low particle concentrations. J Colloid Interface Sci 368(1):319–325
23. Lin MY, Lindsay HM, Weitz DA, Ball RC, Klein R, Meakin P (1989) Universality in colloid aggregation. Nature 339(3):360–362
24. Tsabet EM, Fradette L (2015) Effect of processing parameters on the production of Pickering emulsions. Ind Eng Chem Res 54(7): 2227–2236
25. Bile J, Bolzinger M-A, Vigne C, Boyron O, Valour J-P, Fessi H, Chevalier Y (2015) The parameters influencing the morphology of poly(ε-caprolactone) microspheres and the resulting release of encapsulated drugs. Int J Pharm 494(1):152–166
26. Holmes JM, Beebe RA (1971) Surface areas by gas adsorption on amorphous calcium phosphate and crystalline hydroxyapatite. Calcif Tissue Res 7(1):163–174
27. Yang L, Wei Z, Zhong W, Cui J, Wei W (2016) Modifying hydroxyapatite nanoparticles with humic acid for highly efficient removal of cu(II) from aqueous solution. Colloids Surf A Physicochem Eng Asp 490:9–21
28. Zhu R, Yu R, Yao J, Mao D, Xing C, Wang D (2008) Removal of Cd^{2+} from aqueous solutions by hydroxyapatite. Catal Today 139(1):94–99
29. Vitale-Brovarone C, Miola M, Balagna C, Verné E (2008) 3D-glass-ceramic scaffolds with antibacterial properties for bone grafting. Chem Eng J 137(1):129–136
30. ASTM F 1185–03 (2003) Standard specification for composition of hydroxyapatite for surgical implants. ASTM International, West Conshohocken
31. ASTM F 1088 – 04a (2004) Standard specification for beta-tricalcium phosphate for surgical implantation. ASTM International, West Conshohocken